HYBRID DEEP LEARNING MODEL FOR IMPROVING THE OPERATIONAL EFFICIENCY OF MICROGRIDS

Hong Duy An Nguyen[1], Trong Nhan Van[1], Thi Cat Tuong Nguyen[1], Ngoc Thien Nam Tran[2], Minh Quan Duong[1]*

[1]The University of Danang - University of Science and Technology, Danang city, Vietnam
[2]Delta Electronic, INC, Tainan city, Taiwan

*Corresponding author: dmquan@dut.udn.vn

(Received: April 16, 2025; Revised: May 2, 2025; Accepted: May 28, 2025)

DOI: 10.31130/ud-jst.2025.23(6A).214E

Abstract - Forecasting renewable energy output is crucial for efficient power system operation as their penetration rises. Solar and wind power, highly weather-dependent, require accurate, flexible forecasting methods. This study proposes a hybrid model combining Long Short-Term Memory (LSTM) networks with Inductive Conformal Prediction (ICP) to estimate generation over short-term, medium-term, and long-term horizons. The model not only enhances accuracy but also provides confidence intervals for each forecast, supporting risk-aware decision-making. Simulations based on real-world data from solar and wind plants in Vietnam show that LSTM+ICP significantly outperforms traditional Random Forest Regression (RFR) and LSTM models. Forecast accuracy is evaluated using MAE and RMSE: 0.037/0.097 MW for short-term, 0.178/0.373 MW for week-ahead, and 0.524/0.962 MW for month-ahead forecasts. These results demonstrate the model's ability to reduce systematic error and improve forecast robustness, thereby enhancing operational efficiency and stability of microgrids under highly variable conditions.

Key words - LSTM; improving; microgrid; renewable energy; power forecast

1. Introduction

Amid globalization and rising environmental awareness, transitioning from fossil fuels to renewable energy has become an inevitable trend. Renewable sources such as solar and wind power not only reduce greenhouse gas emissions but also enhance energy security and grid stability. Supportive policies are driving the integration of Renewable Energy Sources (RES), aiming for a more sustainable energy system [1].

Small-capacity RES, along with Distributed Energy Resources (DERs) such as wind power and solar power, are increasingly being integrated into power systems [2]. However, to ensure stable and continuous electricity supply in distribution grids, these systems require accurate power generation forecasting and reliable source assessment [3]. Due to their dependence on natural conditions, the output of renewable energy sources is highly variable: solar power generation is only available when solar irradiance is present, while wind power output fluctuates with wind speed. This variability presents significant challenges for power system operation, especially as the share of renewables in the grid increases, exacerbating supply uncertainty and instability [4]. The concept of microgrids has been developed in recent years to optimize DER integration and enhance renewable energy utilization efficiency. Microgrids enable centralized management and intelligent coordination of distributed generation sources, improving reliability, optimizing grid operations, and supporting the transition to a Smart Grid [5-6].

Deep learning research and its practical applications have been increasingly attracting attention, especially in time series forecasting-an important yet highly challenging problem. Previous studies have primarily focused on supervised learning models such as the Random Forest Regression (RFR) method or simple recurrent neural networks. However, these approaches face significant limitations in handling nonlinear and highly volatile data, particularly in the context of renewable energy power forecasting. Due to the spatial partitioning characteristics of decision trees, RFR fails to exploit the continuity and periodicity in time series data, leading to overfitting in highly fluctuating periods and reduced accuracy in long-term forecasts [7]. On the other hand, while LSTM overcomes RFR’s limitations by utilizing gate mechanisms to retain information over time, this model still has drawbacks, particularly in long-term forecasting. The primary issue is the accumulation of errors over time, where inaccuracies in each prediction step can propagate, reducing the reliability of the overall forecast. Therefore, hybrid models are needed to improve performance [8-9].

The LSTM model, when combined with Inductive Conformal Prediction (ICP), not only handles sequences of variable lengths [10-11] but also quantifies forecast reliability through p-values and confidence intervals. ICP is an advanced statistical method that uses a “calibration” set to assess the level of "nonconformity" of new data compared to the training distribution, thereby determining the probability of deviation for each forecast. By learning the nonlinear relationships between solar radiation, wind speed, and temperature, LSTM+ICP not only provides accurate forecasts but also offers risk assessment alongside predictions. Specifically, ICP utilizes the calibration set to compute nonconformity scores, reflecting the degree of deviation between predictions and actual data. When applied to new data, ICP compares these scores to determine confidence intervals and the reliability of each forecast, thereby optimizing operational decisions in highly volatile conditions [12-13].

This study focuses on evaluating the forecasting performance of LSTM+ICP in predicting renewable energy power output (including solar and wind energy) across short-

, medium-, and long-term horizons. The research results are expected to demonstrate the superiority of LSTM+ICP over LSTM and traditional methods such as RFR in handling the high volatility of renewable energy data. This combination not only improves forecast reliability but also supports power system operators in risk assessment and decision-making under uncertainty, thereby optimizing the operation of renewable energy-integrated power systems.

2. Overall structure and Problem formulation

2.1. Overall structure

The LSTM+ICP model is developed using the Python programming language, with input data sourced from a solar power plant in Đồng Nai province [14] and a wind power plant on Cồn Cỏ Island [15] in Vietnam. This data is used to create a realistic dataset simulating a self-sufficient microgrid capable of integrating into the power system.

Renewable energy sources, such as solar and wind power, are highly influenced by various environmental factors, including solar irradiance, wind speed, air humidity, atmospheric pressure, and temperature. These factors fluctuate rapidly over time and do not follow simple or linear patterns. However, within specific time frames, they exhibit identifiable correlations, forming distinct data distribution patterns, as shown in Figure 1. This inherent instability and nonlinearity present major challenges for traditional power forecasting methods. Earlier forecasting models predominantly relied on basic statistical techniques or linear regression, assuming that the relationships between meteorological inputs and power output could be expressed through linear or simple mathematical functions. However, given the multidimensional complexity and interdependence of meteorological data, these methods often struggle to capture hidden patterns, leading to large forecasting errors and reduced accuracy, especially during sudden weather changes or unpredictable trends.

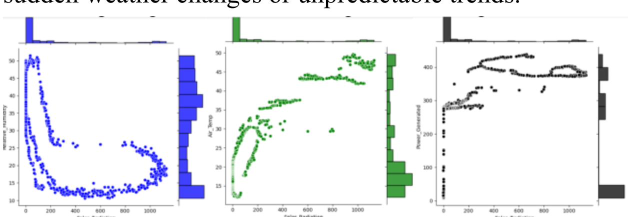

Figure 1. *The chart shows the correlation of input data*

The Long Short-Term Memory (LSTM) recurrent neural network, a powerful deep learning model for time series analysis, has proven to be a highly effective approach for renewable energy forecasting. Unlike traditional models, LSTM retains and processes temporal information over extended periods using its specialized memory mechanism. This capability allows it to capture both short-term fluctuations and long-term patterns in weather data sequences. By learning from historical data, LSTM autonomously identifies and extracts complex relationships, significantly enhancing forecasting accuracy. As a result, this model not only improves the efficiency of renewable energy utilization but also plays a crucial role in optimizing power system operations and mitigating the risks associated with the variability of clean energy sources.

2.2. Overview of the Random Forest Regressor Model

The Random Forest Regressor (RFR) model is a machine learning (ML) technique based on the concept of Random Forest for regression tasks. Fundamentally, RFR aggregates predictions from multiple independent Decision Trees, where each tree is trained on a randomly selected subset of both samples and features. During prediction, the model takes the average of all individual tree outputs to generate the result, as illustrated in Figure 2. By leveraging the "ensemble" approach, RFR mitigates overfitting, which is a common issue when using a single Decision Tree, while also enhancing prediction accuracy.

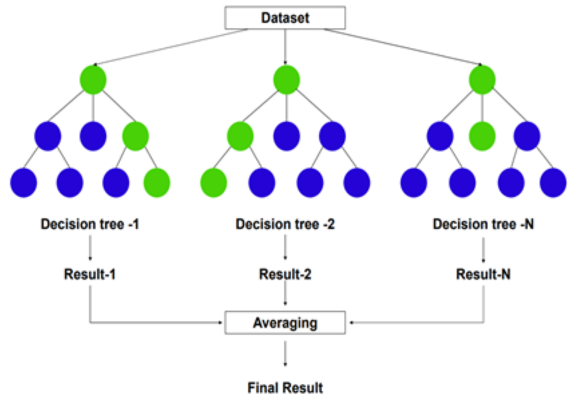

Figure 2. *Structural Diagram of the RFR Model*

2.3. Overview of the LSTM Model

The input data for the model includes solar irradiance, temperature, humidity, wind speed, precipitation, and daylight duration. The output consists of solar and wind power generation capacity. The dataset is structured as a time series, where each timestamp corresponds to specific input parameters and output values at a given point in the day.

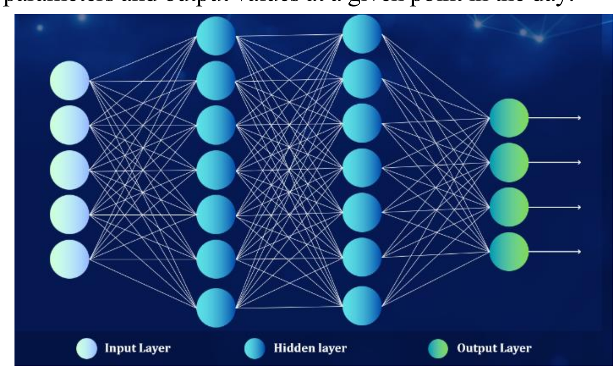

Figure 3. *General Model of the LSTM Network*

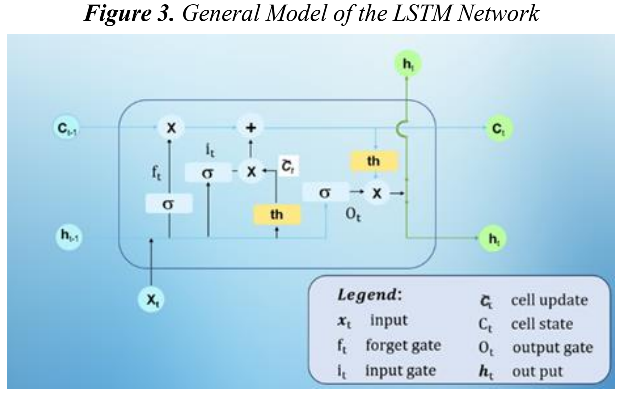

Figure 4. *General Structure of the LSTM Network*

The hidden layers in a LSTM network operate based on a memory and information processing mechanism through four key components: the input gate, forget gate, output gate, and cell state. This architecture enables LSTM to learn and retain long-term dependencies in time series data, enhancing its effectiveness in tasks such as forecasting, sequence classification, and natural language processing.

2.4. Overview of ICP method

ICP is an advanced statistical method in machine learning, developed to add quantitative confidence to model predictions. ICP inherits from the traditional Conformal Prediction (CP) method but improves it by using an inductive process, which significantly reduces the computational cost while maintaining accuracy [13]. The training data is divided into 2 components: Proper training set used to train the base model (LSTM). Calibration set: Used to calculate the non-conformity score. The non-conformity score measures how "different" a sample is from the training set.

2.4.1. Definition of p-value function

$\forall n \in N,\ \forall \delta \in [0,1]$ and for all probability distributions P on Z.

$$P^n\{z \in Z^n : p(z) \leq \delta\} \leq \delta \tag{1}$$

p is semi-computable from above.

This equation ensures that the ICP function constructed has the property of calibration. This means that the probability of the p-value of a sample sequence being less than or equal to δ will not exceed δ

$$\mathrm{p}\,(z_1, \dots, z_n) = \frac{\#\{i=1,\dots,n : \alpha_i \geq \alpha_n\}}{n} \tag{2}$$

Here, α_i is the non-conformity score of the ith sample. This formula calculates the p-value of a sequence by counting the number of samples whose non-conformity score is not smaller than that of the last sample (the new sample to be predicted) and then dividing by the total number of samples n. Consequently, the p-value reflects the "degree of abnormality" of the new sample compared to the training data.

2.4.2. Formula for ICP using a calibration set

$$p(Y_j) = \frac{\#\{i=m+1,\dots,m+q,l+q : \alpha_i \geq \alpha_{l+g}^{(Y_j)}\}}{q+1} \tag{3}$$

This formula allows estimating the “consistency” of the label Y_j for the new example based on the calibration set, without the need to retrain the model for each label [13].

$$\textbf{(-)}\ (U_{train}(l-q) + (q+r)U_{apply}) \tag{4}$$

Here, the model only needs to be trained once on the proper training set (with l−q samples) and then applied to the calibration and test sets. Therefore, ICP significantly reduces computational time compared to CP.

2.4.3. Neural Networks ICP

Applying the ICP method to neural networks for classification problems. The related formulas mainly revolve around defining the non-conformity measure based on the network's output. A common formula when applied to LSTM networks.

$$\alpha_i = \max_{j=1,\dots,c:j\neq u} o_j^i - o_u^i \tag{5}$$

or as

$$\alpha_i = \frac{\max_{j=1,\dots,c:j\neq u} o_j^i}{o_u^i + \gamma} \tag{6}$$

where the parameter γ ≥ 0 in the second definition enables us to adjust the sensitivity of our measure to small changes of o_u^i depending on the data in question. We added this parameter in order to gain control over which category of outputs will be more important in determining the resulting non-conformity scores; by increasing γ one reduces the importance of o_u^i and consequently increases the importance of all other outputs.

2.4.4. The Algorithm

The training data is divided into two parts: the proper training set, used to train the neural network model, and the calibration set, used to calibrate the model by computing non-conformity scores for the samples. After the model is trained on the proper training set to learn data features, each sample in the calibration set is fed into the model to obtain its output and calculate a non-conformity score that reflects how different the sample is from its correct label. When processing a test sample, the model generates output for all possible labels, assuming each label is the correct one, and computes the corresponding non-conformity score. By comparing this score with the calibration set, the algorithm determines a p-value-like measure for each label to assess how well the assumption fits. The label with the highest value, corresponding to the lowest non-conformity score, is chosen as the final prediction. Additionally, the algorithm provides confidence information (based on the second-highest label value) and credibility (based on the predicted label's value). Thus, NN ICP not only makes predictions but also provides certainty measures, helping to evaluate the reliability of the results.

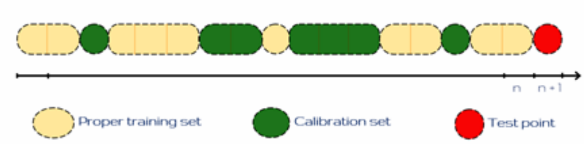

Figure 5. *ICP method*

By providing p-value and confidence interval, it helps to assess the risk of the forecast result, suitable for large training datasets. Therefore, it applies to both classification and regression problems and easily integrates with deep learning models such as LSTM

3. Evaluation method

The forecasting process is performed on a hypothetical area, simulated as a Microgrid. The input data includes weather parameters such as solar radiation, wind speed, temperature, humidity, rainfall, and load consumption, while the output data is the power generation capacity from renewable energy sources (solar and wind). These parameters are used to calculate the Pnetload value, determined by the formula: $P_{netload} = P_{load} - P_{solar} - P_{wind}$.

The main objective of the study is to compare the deviation between the forecasted Pnetload value and the actual value, thereby evaluating the performance of the LSTM+ICP, LSTM, and RFR models (representing the traditional method) in forecasting renewable energy capacity. In all evaluation time frames, the same dataset is used to ensure consistency when comparing forecasting methods.

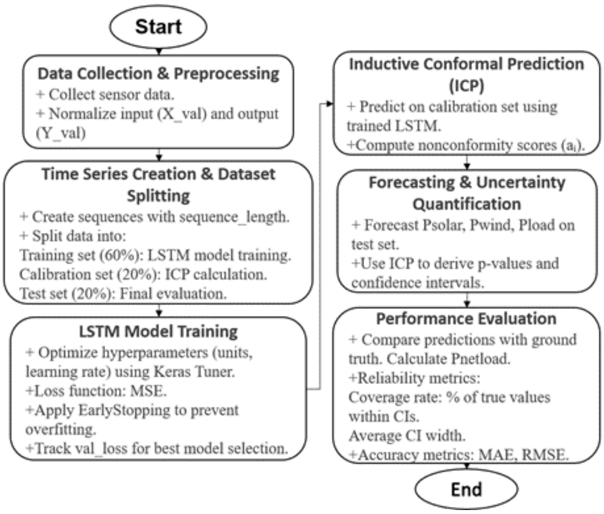

Figure 6. *Block diagram of training and energy forecasting process with LSTM*

The study performed Pnetload forecasting on three different time frames: short-term (24 hours), medium-term (1 week), and long-term (1 month). Each time frame serves different purposes in power system operation management as mentioned in [16]

Short term: Support real-time operation dispatching and rapid power adjustment.

Medium-term: Provide flexible dispatch information to help plan weekly power allocation.

Long-term: Support long-term strategic planning, optimize power system operations, and ensure energy security.

The accuracy of the forecasts in each time frame is evaluated based on two important indicators: Mean Absolute Error (MAE) and Root Mean Square Error (RMSE). The statistical analysis results help determine the level of error of each model, thereby making judgments about the effectiveness of the forecasting methods.

Table 1. *Evaluation time frames [16]*

Time frame	Time period (time step =15 min)
Short term	24 hours
Medium-term	1 week
Long term	1 month

4. Simulation results and discussion

4.1. Forecast results for 3-time frames

Based on Figure 7, the forecast results in the graph as well as the MAE and RMSE (Table 2) indexes from the three models RFR, LSTM, and LSTM+ICP all closely follow the actual load curve, but the degree of agreement is different. With RFR, the forecast curve is relatively consistent most of the time, but there are still some significant differences when the capacity changes suddenly. Meanwhile, the LSTM model has shown a clear improvement in smoothness and adherence to the actual curve, especially in the fast-varying sections. Finally, the LSTM model combined with the ICP mechanism (LSTM+ICP) shows the forecast results closest to the actual data, maintaining stability in both stable and fast-varying data regions.

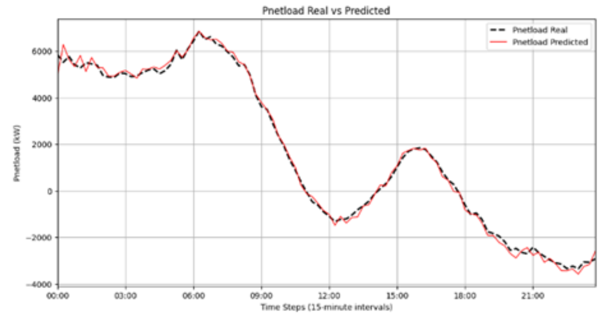

a) RFR model

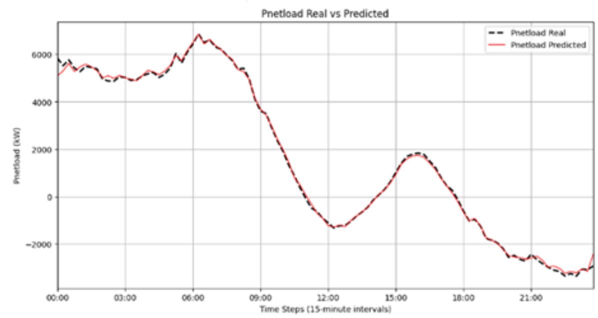

b) LSTM model

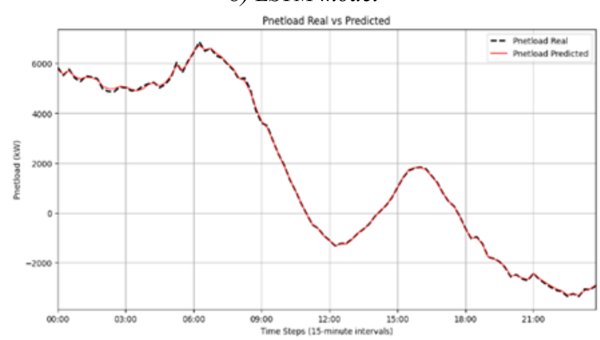

c) LSTM+ICP model

Figure 7. *Comparison graph of actual $P_{netload}$ and forecast $P_{netload}$ for the next 24 hours*

Looking at Figure 8, although the deviation is greater than the forecast for the next day, all three methods still follow the actual power curve quite well. In particular, the RFR model gives good results in the power segments that do not change too quickly, but the overfitting level is quite high in some time periods and has a higher tendency to overfit than LSTM and LSTM+ICP. The LSTM model is more sensitive to rapid changes in power, so it significantly reduces the phase difference between the forecast value and the actual value, especially at the peaks and troughs of the curve. Finally, the LSTM model with ICP (LSTM+ICP) shows more stable forecasting ability, especially in the transition periods, thanks to the addition of information correction and forecast control mechanisms.

Based on Figure 9, all three models follow the capacity evolution relatively well throughout the following month, but the accuracy is not very high. The limitations of each model also become clearer. Therefore, long-term forecasting is only suitable to support managers and policymakers in assessing market trends, predicting consumption demand, and adjusting power system development planning, thereby optimizing resource allocation and minimizing economic and technical risks in the long term.

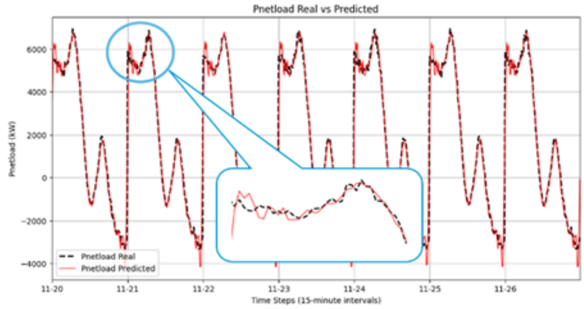

a) RFR model

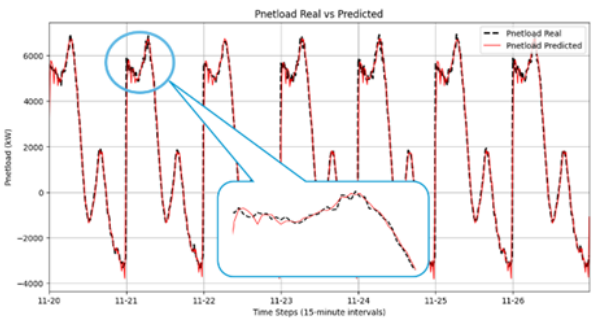

b) LSTM model

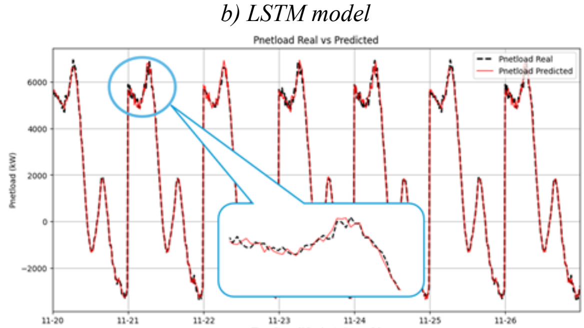

c) LSTM+ICP model

Figure 8. *Comparison graph of actual $P_{netload}$ and forecast $P_{netload}$ for the next week*

Based on the forecasting curves presented in Figures 7, 8, and 9 and the MAE and RMSE indices presented in Table 2, the LSTM and LSTM+ICP models are capable of closely following the actual trend of Pnetload, especially in cases of unusual fluctuations due to weather. LSTM+ICP not only closely follows the actual trend but also provides confidence intervals for risk assessment, which other models do not have. The forecasting curve of LSTM+ICP responds faster to sudden changes while maintaining high accuracy thanks to the ability to eliminate unreliable predictions.

In contrast, the forecasted curve of the RFR model tends to be smoother and exhibits fewer fluctuations at points where weather conditions change abruptly. This leads to deviations during periods of high volatility. Moreover, when dealing with a large dataset containing numerous parameters and sudden variations, RFR is more prone to overfitting compared to LSTM and LSTM+ICP if appropriate adjustments are not applied. The primary reason lies in RFR, which is based on an ensemble of decision trees, limiting its adaptability to rapidly changing time series data. While this characteristic helps reduce noise in predictions, it also results in the loss of crucial data points that reflect the actual trends in the dataset.

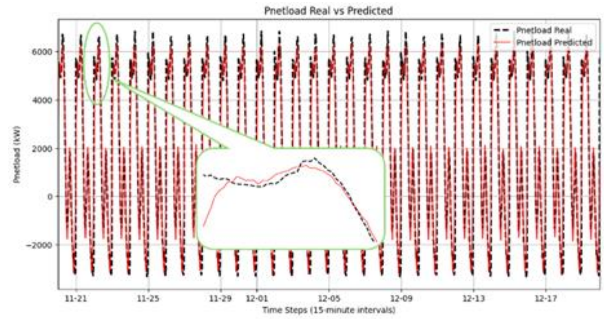

d) RFR model

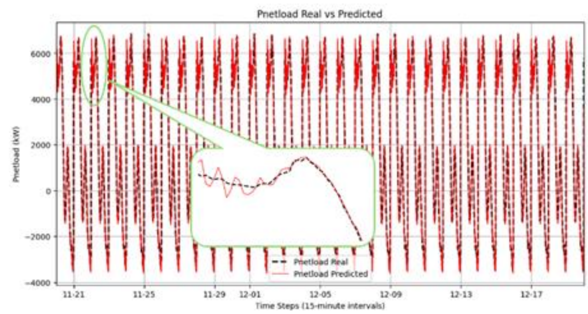

e) LSTM model

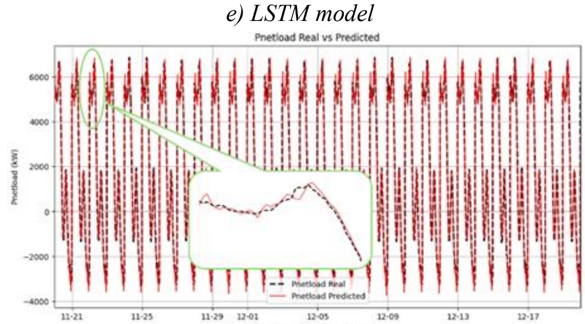

(k) LSTM+ICP

Figure 9. *Comparison graph of actual $P_{netload}$ and forecast $P_{netload}$ for the next month*

4.2. Comparison of model parameters using MAE and RMES indexes

To evaluate the forecasting accuracy of the above methods, the selected evaluation metrics include RMSE and MAE. These metrics are commonly used to measure the deviation between the model's predictions and observed values, with smaller values indicating lower errors.

$$RMSE = \sqrt{\frac{1}{N}\sum_{t=1}^{N}(y_t - \widehat{y_t})^2} \quad (7)$$

$$MAE = \frac{1}{N}\sum_{t=1}^{N}(|y_t - \widehat{y_t}|) \quad (8)$$

In the formula, N is the total number of samples, y_t is the actual observation value; k is the number of independent variables, $\widehat{y_t}$ is the predicted value; $\overline{y_t}$ the mean of actual observations.

***Table 2.** MAE and RMES indexes in time frames*

	Time frame	MAE(MW)	RMES(MW)
RFR	Short term	0.173	0.362
	Medium-term	0.423	0.894
	Long term	1.264	2.534
LSTM	Short term	0.102	0.224
	Medium-term	0.283	0.513
	Long term	0.924	1.749
LSTM+ICP	Short term	0.037	0.097
	Medium-term	0.178	0.373
	Long term	0.524	0.962

The comparison table of MAE and RMSE shows that, when considering the three forecasting models (RFR, pure LSTM, and LSTM combined with ICP), the LSTM+ICP model has the best performance in all time frames. Specifically, in the short term (24 hours), LSTM+ICP achieves MAE = 0.037 MW and RMSE = 0.097 MW, which is significantly lower than pure LSTM (MAE = 0.102 MW, RMSE = 0.224 MW) and RFR (MAE = 0.173 MW, RMSE = 0.362 MW). This shows that the ability to memorize and react quickly to LSTM, thanks to the gate mechanism, has been enhanced by an additional step of forecast correction through ICP, helping to compensate for systematic errors. In contrast, RFR has a higher error due to the characteristics of this model that do not take advantage of the continuity and periodicity in time series data.

In the medium (1 week) and long (1 month) term, although both LSTM and RFR tend to decrease in accuracy with the forecasting horizon, LSTM+ICP still maintains its superiority. This performance degradation reflects the complexity and unpredictability of time series data as the forecast horizon increases. RFR, with its structure based on decision trees, performs better on data with clear structures or simple relationships but has difficulty modeling complex long-term correlations.

These results show that RFR fails to take advantage of the continuity and periodicity of time series data, resulting in smooth forecasts that miss important fluctuations. Meanwhile, the pure LSTM model, thanks to the gate mechanism, can remember short-term and long-term dependencies, helping to catch up with sudden fluctuations. However, when combined with ICP, the LSTM model not only maintains the advantages of LSTM but also allows for forecast error correction by using the calibration set to calculate non-conformance points. Thereby, LSTM+ICP provides more accurate forecast intervals and reduces forecast errors (MAE, RMSE) compared to both other models.

5. Conclusion

LSTM has proven its superiority in forecasting renewable energy output thanks to its ability to learn nonlinear relationships and capture strong fluctuations in time series data. When combined with ICP, the LSTM+ICP model not only enhances accuracy but also provides confidence intervals, enabling forecast adjustments and supporting decision-making. In the short and medium term, LSTM+ICP maintains stable performance and minimizes systematic errors. However, in the long term, both LSTM and LSTM+ICP may be affected by error accumulation and uncertainties. To address this, model optimization or integration with advanced methods like Transformer, which effectively handles long-term dependencies through the self-attention mechanism, is necessary. Overall, DLSTM+ICP is a promising solution that enhances forecast reliability and supports more effective power system management.

Acknowledgments: This research is funded by the Funds for Science and Technology Development of the University of Danang under project number B2023-DN01-03.

REFERENCES

[1] J. E. Kim and T. Tang, "Preventing early lock-in with technology-specific policy designs: The Renewable Portfolio Standards and diversity in renewable energy technologies", *Renewable and Sustainable Energy Reviews*, vol. 123, no. 3, pp. 109738, 2020.

[2] M. Q. Duong, N. T. Nam Tran, G. N. Sava, and M. Scripcariu, "The impacts of distributed generation penetration into the power system", in *Proc. Int. Conf. Electromechanical and Power Systems (SIELMEN)*, Iasi, Romania, 2017, pp. 295–301.

[3] S. Ahmad, *et al.,* "A review of microgrid energy management and control strategies", *IEEE Access*, vol. 11, 2023.

[4] N. T. N. Tran, M. Q. Duong, and H. T. Yang, "Integrated Transient Stability Analysis with Multi-Large-Scale Solar Photovoltaic in Distribution network", *Journal of Science and Technology*, vol. 147(C), pp. 40–45, 2020.

[5] T. B. Nadeem, *et al.,* "Distributed energy systems: A review of classification, technologies, applications, and policies", *Energy Strategy Reviews*, vol. 48, 2023.

[6] C. L. Smallwood, "Distributed generation in autonomous and nonautonomous micro-grids", in *Proc. Rural Electric Power Conf.*, Colorado Springs, CO, USA, pp. D1-1–D1-6, May 2002.

[7] R. I. Mukhamediev, et al., "Review of artificial intelligence and machine learning technologies: Classification, restrictions, opportunities and challenges", *Mathematics*, vol. 10, no. 15, pp. 2552, 2022.

[8] N. L. M. Jailani *et al.*, "Investigating the Power of LSTM-Based Models in Solar Energy Forecasting", *Processes*, vol. 11, pp. 1382, 2023.

[9] K. A. Althelaya, E. M. El-Alfy, and S. Mohammed, "Evaluation of bidirectional LSTM for short-and long-term stock market prediction", in *Proc. Int. Conf. Information and Communication Systems (ICICS)*, 2018.

[10] X. Yang, *et al*., "Evaluation and interpretation of runoff forecasting models based on hybrid deep neural networks", *Water Resources Management*, vol. 38, no. 6, 2024.

[11] M. Mohammadi, *et al.,* "Advanced fusion of MTM-LSTM and MLP models for time series forecasting: An application for forecasting the solar radiation", *Measurement: Sensors*, vol. 33, 2024.

[12] L. Zhu, *et al.,* "A novel U-LSTM-AFT model for hourly solar irradiance forecasting", *Renewable Energy*, vol. 238, pp. 121955, 2025.

[13] H. Papadopoulos, V. Vovk and A. Gammerman, "Conformal prediction with neural networks", in *Proc. 19th IEEE Int. Conf. Tools with Artificial Intelligence (ICTAI)*, 2007.

[14] Huawei, "Energy Report of LK Power Station 1 for April 2024", *FusionSolar,* Apr 30, 2024. [Online]. Available: https://sg5.fusionsolar.huawei.com/ [Accessed: Jun. 22, 2025].

[15] V. T. Le, *"Study on the Development of a Wind Power System for Con Co Island District, Quang Tri Province"*, Master's thesis, The University of Danang - University of Science and Technology, Danang City, Vietnam, 2017.

[16] C. Sweeney, R. J. Bessa, J. Browell, and P. Pinson "The future of forecasting for renewable energy", *Wiley Interdisciplinary Reviews: Energy and Environment*, vol. 9, no. 2, pp. e365, 2020. DOI: 10.1002/wene.365